Electronic Supplementary Information

Deformability-Based Cell Classification and Enrichment Using Inertial Microfluidics

Soojung Claire Hur[1,2], Nicole K. Henderson-MacLennan[3], Edward R.B. McCabe[4], Dino Di Carlo[2,5]

1 Mechanical and Aerospace Engineering Department, University of California Los Angeles, Los Angeles, CA, USA 90095
2 California NanoSystems Institute, Los Angeles, CA, USA 90095
3 Department of Pediatrics, David Geffen School of Medicine, University of California Los Angeles, Los Angele, CA, USA 90095
4 Department of Pediatrics, Linda Crnic Institute for Down Syndrome, Aurora, CO USA 80045
5 Department of Bioengineering, University of California Los Angeles, Los Angeles, CA, USA 90095

Table of Contents

ELECTRONIC SUPPLEMENTARY INFORMATION FIGURES

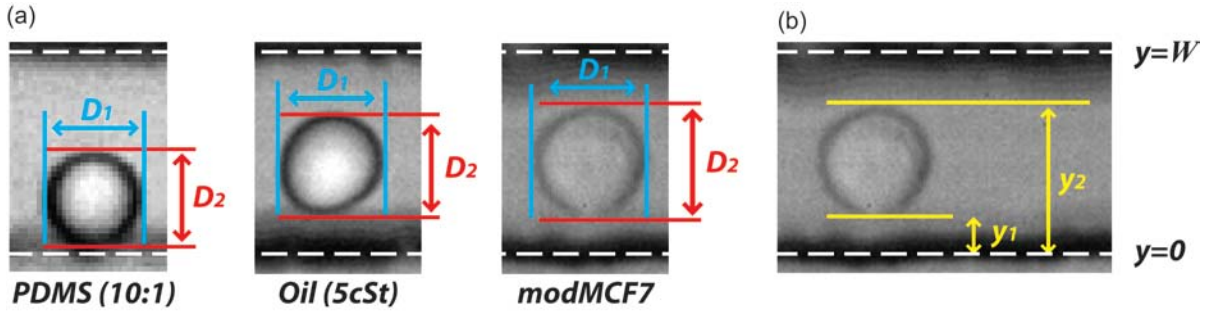

ESI_Figure 1 Measurements of diameter and lateral equilibrium position. (a) Diameter, *a*, of particles, droplets and cells was determined by measuring and averaging the distance between outer edges of particulates in lateral (D_1) and vertical (D_2) directions ($a = (D_1+D_2)/2$). (b) Lateral equilibrium positions of flowing particulates were determined from the distance of the center position from the wall ($X_{eq} = (y_1+y_2)/2$).

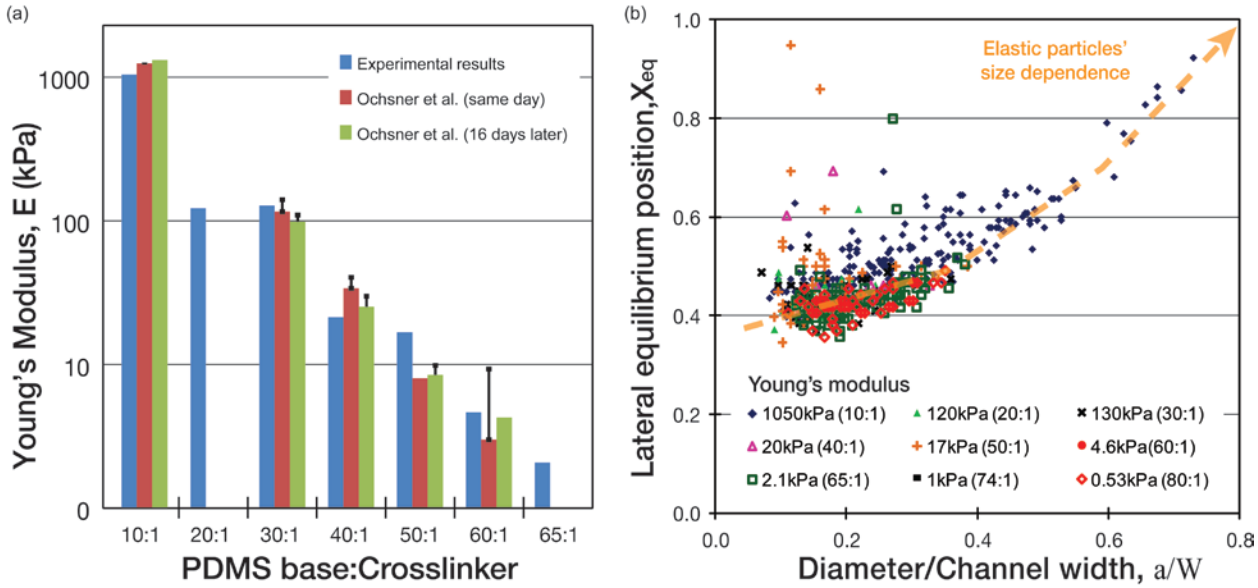

ESI_Figure 2 Young's Modulus of PDMS particles and its effect on lateral equilibrium position. (a) Elasticity of bulk PDMS specimens was controlled by varying crosslinker density and their Young's modulus was measured using the standard tensile test (Instron 4111, elongation rate at 0.5mm/min). The measured values were in good agreement with those reported by Ochsner *et al.*[1]. (b) The inertial focusing equilibrium positions (X_{eq}) of PDMS particles ($2 < a < 20\mu m$) was found to depend on particle size but was independent of elasticity over the range tested. It can be attributed that deformation of elastic solid particles was not sufficient enough to induce the lateral drift force, as previously theoretical analysis discussed[2].

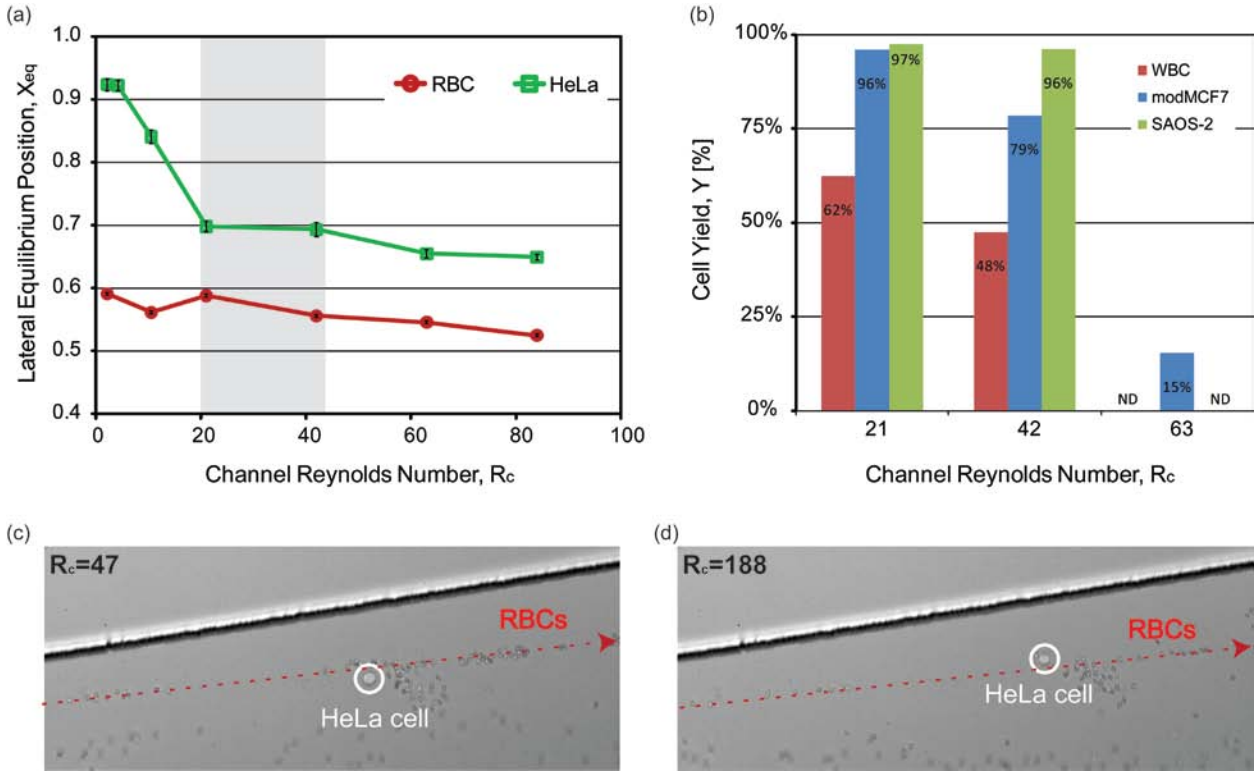

ESI_Figure 3 Experimental assessments to determine optimum condition for label-free cancer cell enrichment based on cell deformability. (a) The lateral equilibrium position of human red blood cells and HeLa was found to be decreasing with increasing channel Reynolds number, R_c. Error bars indicate the standard error. (b) The number of cells collected at cancer (three inner) outlets was found to be decreasing as R_c increases. The yield of WBC and SAOS-2 collected at R_c =63 was not determined (marked as ND) since that of modMCF7 was found to be impractical for enrichment purposes. Thus, optimum flow rate (shadowed region in part (a)) that would allow the maximum cancer cell enrichment was decided to be $20 < R_c < 42$. The error bar in part (a) indicates the standard error (N=100). (c) More deformable cancer cells, initially focused closer to the channel centerline in the straight channel, remained closer to the channel centerline than RBCs at the expanding outlet. (d) Cancer cells and blood cells, however, had unexpected but distinct paths at the expanding outlet when the mixture was injected at high rates, suggesting the importance of the outlet geometry.

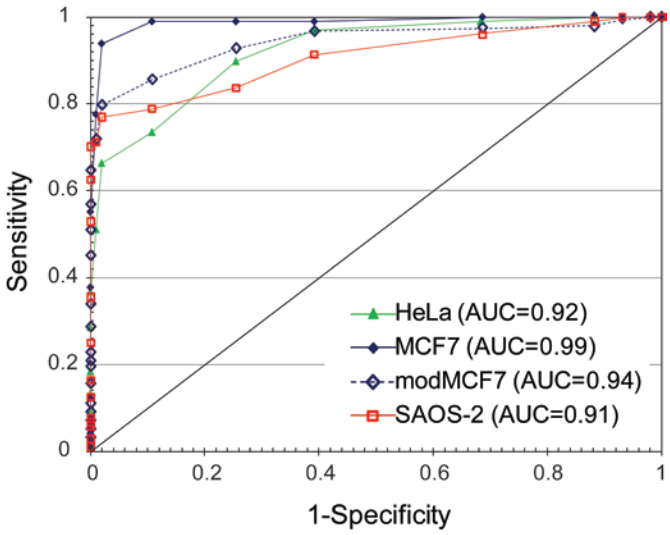

ESI_Figure 4 Receiver operating characteristic (ROC) curve, graphically representing the sensitivity and specificity of the current technique for cancer cell classification from blood samples. Each point on the ROC curve corresponds to all possible lateral equilibrium position thresholds ($0.4 < X_{eq} < 1$ with 0.02 interval). Full area under the ROC curve (AUC), the accuracy index of the current technique, was determined using the empirical methods[3]. The detection technique with perfect sensitivity and specificity would have AUC value equal to 1. A high AUC (greater than 0.91) was attained for all cancer cell types, indicating that the current technique would enable cancer cell detection from patient's blood sample with high sensitivity and specificity.

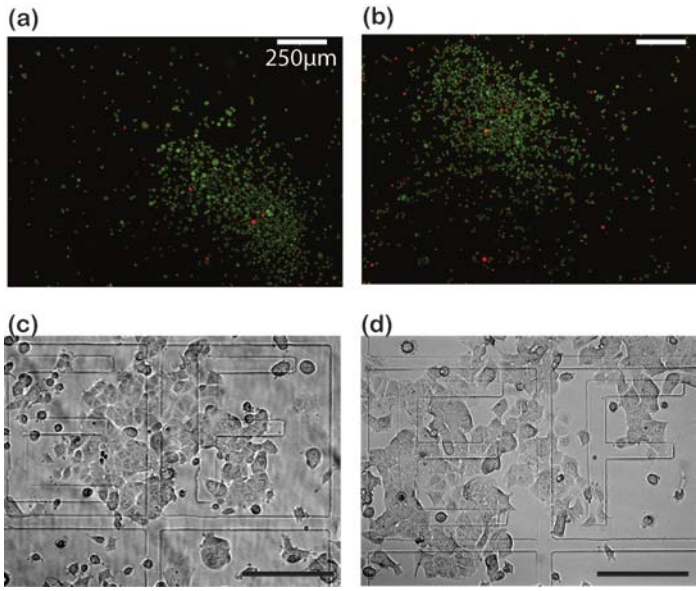

ESI_Figure 5 Processed cancer cells remain highly viable. Fluorescent microscopic images of (a) control and (b) MCF7 cells flowed through stained with Calcein AM/Ethidium homodimer-2 show that processed cells are highly viable. Microscopic images of (c) Control and (d) processed MCF7 cells at day 7. Both cells were plated on petri-dishes with grid (ibidi) and cultured over a week and flowed cells proliferated well with similar morphology as control sample. Scale bars are 250µm.

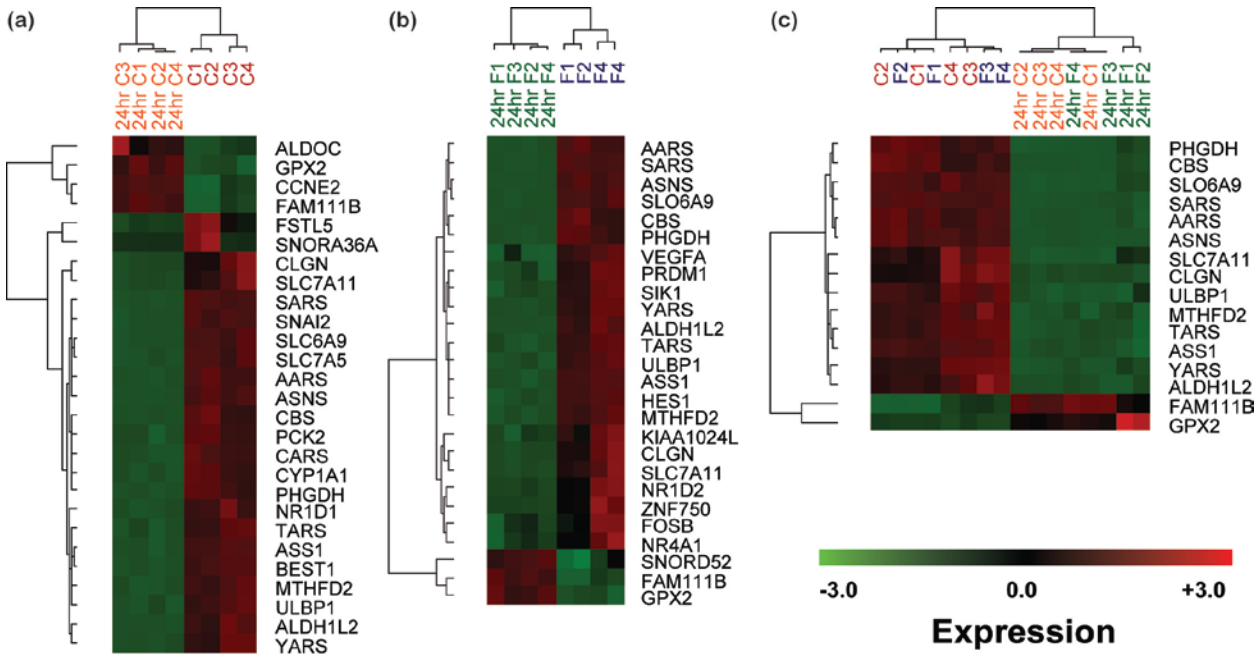

ESI_Figure 6 Hierarchical clustering dendogram of gene lists illustrates the temporal difference between (a) control and 24hour control, (b) flowed and 24hour flowed, and (c) control vs. 24hour control and flow vs. 24hour flow samples. These three gene lists were used for pathway/function analysis.

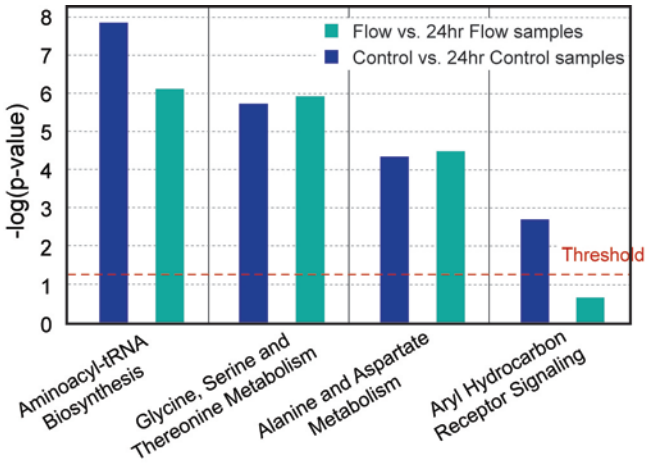

ESI_Figure 7 Pathway analysis of temporal effect on gene expression of MCF7 cells. Three significant canonical pathways were found to be in common in both control vs. 24hour control and flow vs. 24hour flow samples, suggesting minor alteration in gene expression is independent of flowing cells through the device.

ELECTRONIC SUPPLEMENTARY INFORMATION MOVIE

ESI_Movie 1 Deformability Activated Cell Soring (DACS) device. modMCF7 cells spiked in dilute blood (0.5% hematocrit) flowing at Q = 55µl/min (R_c=21).

REFERENCE

1. Ochsner, M. et al., *Micro-well arrays for 3D shape control and high resolution analysis of single cells, Lab Chip* **7** (8), 1074 (2007).
2. Tam, C. K. W. and Hyman, W., *Transverse motion of an elastic sphere in a shear field, Journal of Fluid Mechanics* **59**, 177 (1973).
3. Lasko, T., Bhagwat, J., Zou, K., and Ohno-Machado, L., *The use of receiver operating characteristic curves in biomedical informatics, Journal of Biomedical Informatics* **38** (5), 404 (2005).